ORIGINAL ARTICLE

A C G publications

Bioorg. Med. Chem. Rep. 8:1 (2025) 10-27

Bioorganic & Medicinal Chemistry Reports

In silico prediction of some peroxisome proliferator-activated receptor (PPAR) agonists targeted drugs as potential SARS-CoV-2 inhibitors

Suleyman Akocak[1*], Erkan Öner[2], Gökçenur Gürbüz[3] and Nebih Lolak[1]

[1]*Adıyaman University, Faculty of Pharmacy, Department of Pharmaceutical Chemistry, 02040, Adıyaman, Türkiye*
[2] *Adıyaman University, Faculty of Pharmacy, Department of BioChemistry, 02040, Adıyaman, Türkiye*
[3]*Adıyaman University, Faculty of Pharmacy, 02040, Adıyaman, Türkiye*

(Received March 06, 2025; Revised June 07, 2025; Accepted June 23, 2025)

Abstract: Since COVID-19 epidemic began, no effective medication have been found to treat this disease. In the current study, several peroxisome proliferator-activated receptor (PPAR) agonist drugs, including fenofibrate, binifibrate, bezafibrate, ciprofibrate, clofibrate, gemfibrozil, pioglitazone, and rosiglitazone were selected, and the molecular docking studies were applied by using main protease (M^{pro}), human angiotensin-converting enzyme 2 (ACE2), and transmembrane protease serine 2 (TMPRSS2) targets. The chemical structures of selected drugs were retrieved from the PubChem database (https://pubchem.ncbi.nlm.nih.gov/). AutoDock 4.2 molecular docking program was used to obtain best binding interactions of selected drugs. Visualization of the docking results was performed using BIOVIA Discovery Studio Visualizer and PyMol. As a result, rosiglitazone and binifibrate were found to be an effective drugs against SARS-CoV-2 main protease (M^{pro}) with binding energies of –6.8 and -6.7 kcal/mol, respectively. Bezafibrate and binifibrate were found to be an effective drugs against ACE2 with binding energies of -8.6 kcal/mol, respectively. On the other hand, fenofibrate, bezafibrate and rosiglitazone showed highest binding energies against TMPRSS2 protein as compared with reference drugs favipiravir, chloroquine, and hydroxychloroquine. Our *in silico* results suggest that PPAR agonist drugs warrant further investigation as potential lead molecules for discovering more potent compounds in anti-CoV drug development research.

Keywords: SARS-CoV-2; molecular docking; ACE2; TMPRSS2.

1. Introduction

In December 2019, the world faced a new pandemic with the detection of serious pneumonia cases in Wuhan, Hubei province, China.[1] The outbreak was attributed to a new coronavirus (SARS-CoV-2) due to its similarity with one of the previously known coronaviruses, SARS-CoV, and the disease was named coronavirus disease 2019 (COVID-19).[2,3] The epidemic spread to almost all parts of the world in a short time.[4,5]

Coronaviruses are viruses in the genus *Betacoronavirus* belonging to the Coronaviridae family.[6] They are also large, globular, single-stranded and enveloped RNA viruses. This virus consists of spike protein (S), membrane protein (M), envelope protein (E), and nucleocapsid protein (N). The S, M, and

* Corresponding author: E-mail: akocaksuleyman@gmail.com

The article was published by ACG Publications
http://www.acgpubs.org/journal/bioorganic-and-medicinal-chemistry-reports January-June 2025 EISSN: 2667-6028
DOI: http://doi.org/10.25135/bmcr.34.2502.3426
Available online: June 30, 2025

E proteins are embedded in the viral envelope, while the N protein protects the viral RNA genome.[7] Entry of the virus into the host cell is mediated by S proteins.[8] The S protein consists of S1 and S2 subunits. The receptor binding site is located in the S1 subunit on the cell surface. The S2 subunit functions to prepare the S protein by the proteases required for the virus to enter the cell.[9] The main receptor required for SARS-CoV-2 to enter the host cell via S proteins is angiotensin-converting enzyme 2 (ACE2), which is abundant in lung epithelial cells, small intestinal enterocytes, and arterial and venous endothelial cells.[10,11] For the virus enter the host cell, the virus's S protein must undergo various proteolytic cleavages related to the S1 and S2 subunits after binding to its receptor in the host cell. After these proteolytic cleavages, the embedded S protein rises to the cell surface and initiates virus entry into the cell.[6,12] Various host proteases are involved in carrying out these cleavage processes and these proteases exert increased effects on transmission of infection by assisting the entry of the S protein into the host cell. TMPRSS2, acting as one of these proteases, plays an important role in ACE2 and S1/S2 proteolytic divisions, a critical step in allowing SARS-CoV-2 to enter the cell, and helps the virus to spread.[13] ACE2 and TMPRSS2 co-locate on the cell surface, increasing viral entry into the host cell.[14]

Peroxisome proliferator-activated receptor (PPAR) agonists, belonging to the nuclear receptor superfamily, are transcription factors involved in various metabolic pathways in the organism, including glucose and lipid metabolism, energetic homeostasis, cell differentiation and proliferation. Upon ligand binding, peroxisome proliferator-activated receptor migrate to the nucleus, where they heterodimerize with the retinoid X receptor and exert their effects by binding to peroxisome proliferator response elements to regulate transcription of target genes. There are 3 isoforms of these transcription factors, including PPARα, PPARγ, and PPARβ/δ.[15] Various agonists of these isoforms represent important pharmacological tools that provide beneficial therapeutic effects in various metabolic diseases such as diabetes and atherosclerosis.[16] PPARα controls fatty acid transport, fatty acid oxidation and ketogenesis.[17] In particular, PPARα agonists such as fenofibrate, bezafibrate and gemfibrozil are used as antihyperlipidemic drugs. These drugs show the regulatory effects of the lipid profile in the organism.[18,19] PPARγ is the main regulator of adipogenesis, which can increase insulin sensitivity and glucose metabolism.[17] PPARγ agonists such as rosiglitazone and pioglitazone are important drug groups with antidiabetic effects.[20] PPARβ/δ increases lipid and glucose metabolism and regulates energy metabolism.[17] Also, in addition to their ability to induce significant metabolic changes, PPAR agonists have been recently studied for their different repurposing, including their anti-tumor effects.[21,22]

Considering that drug development methods are quite expensive and time-consuming, investigating an existing drug for a repurposing can be beneficial in terms of time and economy.[23] It is a desirable strategy to use an existing drug for repurposing or to evaluate the possible pleiotropic effects of an approved drug, especially in diseases such as COVID-19 where an emergency treatment strategy should be developed. Therefore, *in silico* evaluation of the effects of existing drugs for different targets in the treatment of SARS-CoV-2 disease will be a prediction for both economic and future studies.[24-26] One of the best-characterized drug targets among coronaviruses is the main protease (M^{pro}), and because of its important roles in viral replication, *in silico* trials of many drugs are focused on this protease.[27,28] In this study, we investigated the binding activities of various PPAR agonists to SARS-CoV-2 M^{pro}, ACE2 and TMPRSS2, taking into account the receptors and proteases that play an important role in the entry of SARS-CoV-2 into the host cell. The high-affinity binding activities of these compounds will provide fundamental information for further clinical trials and improve structure-based drug discovery against SARS-CoV-2.

2. Experimental

The AutoDock 4.2 molecular docking program was used to obtain best binding interactions of selected PPAR agonist drugs against SARS-CoV-2 M^{pro}, ACE2, and TMPRSS2. The three-dimensional (3D) structures of SARS-CoV-2 M^{pro} (PDB ID: 6LU7),[29] ACE2 (PDB ID: 1R4L),[30] and TMPRSS2 (PDB ID: 7MEQ)[31] structures were retrieved from the RCSB (Research Collaboratory for Structural Bioinformatics) Protein Data Bank (https://www.rcsb.org/). The drugs that used in the current work is fenofibrate, binifibrate, bezafibrate, ciprofibrate, clofibrate, gemfibrozil, pioglitazone, and rosiglitazone. Also, favipiravir, chloroquine, and hydroxycholoroquine was used as standard drugs for comparison. The 3D chemical structures of these drugs were obtained in sdf format from the PubChem database

(https://pubchem.ncbi.nlm.nih.gov/). The Avogadro 1.2 software was used to transform their 3D structures to PDB format, and all of the structures were energy reduced, torsion of the ligands was examined and then the files converted PDBQT format by using AutoDock tools. The most suitable of the possible binding modes obtained as a result of the Molecular Docking processes were determined with Autodock 4.2, and their analyzes and visuals were obtained with the BIOVIA Discovery Studio Visualizer 2020 program.[32-36] Grid generations were computed by blind docking approach and it was applied all of the docking studies. Lamarckian Genetic Algorithm was used by the 300 individuals in population, 2 500 000 maximum energy evaluations, and 54 000 maximum generations as docking settings to give 100 runs. The lowest docked binding free energy was evaluated the optimal conformations for each docking procedure by using BIOVIA Discovery Studio Visualizer and PyMOL to create the final figures of the docked structure.

3. Results and Discussion

The docking analysis result of the molecules and standards (fenofibrate, binifibrate, bezafibrate, ciprofibrate, clofibrate, gemfibrozil, pioglitazone, rosiglitazone, favipiravir, chloroquine, and hydroxycholoroquine) as inhibitors of SARS-CoV-2 M^{pro} (PDB ID: 6LU7),[29] ACE2 (PDB ID: 1R4L),[30] and TMPRSS2 (PDB ID: 7MEQ)[31] including binding energy (kcal/mol) and inhibition constants are illustrated in Table 1. Additionally, hydrogen bonds (H-bonds), some important hydrophobic interactions and electrostatic interactions are shown in Table 2.

In this study, various PPAR agonist drugs were selected and docked in the active site of SARS-CoV-2 M^{pro}, ACE2 and TMPRSS2 to identify the best drugs among them. For this purpose, favipiravir, chloroquine and hydroxychloroquine were also used as standard drugs for comparison. As can be seen in Table 1, the best binding energy poses against SARS-CoV-2 M^{pro} (PDB ID: 6LU7), ACE2 (PDB ID: 1R4L) and TMPRSS2 (PDB ID: 7MEQ) were observed with chloroquine with -7.2, -8.3, and -6.0 kcal/mol, respectively. The compounds showing binding affinity close to chloroquine to SARS-CoV-2 M^{pro} (PDB ID: 6LU7) were rosiglitazone and binifibrate. The least binding was observed with clofibrate but all compounds showed effective binding affinity results compared to favipiravir. Among them, the amino acid binding and distances of the docking results are presented in Figure 1. Target site dockings to SARS-CoV-2 M^{pro} are also shown in Figure 2. In SARS-CoV-2 M^{pro} (PDB ID: 6LU7), the docking scores were as follows: Chloroquine>Rosiglitazone>Binifibrate>Pioglitazone>Fenofibrate=Bezafibrate>Hydroxychloroquine>Ciprofibrate>Gemfibrozil>Clorofibrate>Favipiravir

In ACE2 (PDB ID: 1R4L), chloroquine and hydroxychloroquine compounds showed good results. Compared to chloroquine and hydroxychloroquine compounds, binifibrate and bezafibrate compounds showed better binding affinity while fenofibrate showed close binding affinity with pioglitazone, rosiglitazone and gemfibrozil compounds. The least binding was observed with clofibrate. The distances of amino acid binding and docking results are presented in Figure 3. ACE2 target site dockings are also shown in Figure 4. In ACE2 (PDB ID: 1R4L), the docking scores were as follows, respectively:Binifibrate=Bezafibrate>Chloroquine>Hydroxychloroquine>Fenofibrate>Pioglitazone>Rosiglitazone>Gemfibrozil>Ciprofibrate>Clofibrate=Favipiravir.

TMPRSS2 (PDB ID: 7MEQ) also showed good binding affinity between chloroquine and hydroxychloroquine standard drugs. When chloroquine and hydroxychloroquine were compared with our targeted ligands, fenofibrate, binifibrate, bezafibrate, gemfibrozil, pioglitazone, rosiglitazone compounds showed better binding affinity, while ciprofibrate and clorofibrate compounds showed lower binding affinity. Amino acid binding distances and docking results are presented in Figure 5. ACE2 target site dockings are also shown in Figure 6. The docking scores in TMPRSS2 (PDB ID: 7MEQ) were as follows, respectively:

Fenofibrate=Bezafibrate>Gemfibrozil>Binifibrate=Pioglitazone>Chloroquine>Hydroxychloroquine>Ciprofibrate>Clofibrate>Favipiravir.

Table 2 shows the target bond structures of fenofibrate, binifibrate, bezafibrate, ciprofibrate, clofibrate, gemfibrozil, pioglitazone, rosiglitazone, favipiravir, chloroquine, and hydroxycholoroquine in SARS-CoV-2 M^{pro} (PDB ID: 6LU7), ACE2 (PDB ID: 1R4L) and TMPRSS2 (PDB ID: 7MEQ), protein structures.

Table 1. Binding energy scores and inhibition constants of drugs against SARS-CoV- 2 M^{pro} (PDB ID: 6LU7), ACE2 (PDB ID: 1R4L), and TMPRSS2 (PDB ID: 7MEQ) by molecular docking study.

Protein	Drugs	Binding Energy (kcal/mol)	Inhibition Constant
6LU7	Fenofibrate	-6.4	6.01 µM
	Binifibrate	-6.7	12.40 µM
	Bezafibrate	-6.4	23.14 µM
	Ciprofibrate	-6.0	92.93 µM
	Clofibrate	-5.1	57.68 µM
	Gemfibrozil	-5.7	54.683µM
	Pioglitazone	-6.5	11.16 µM
	Rosiglitazone	-6.8	11.96 µM
	*Favipiravir	-4.2	815.53 µM
	*Chloroquine	-7.2	5.10 µM
	*Hydroxychloroquine	-6.3	25.82 µM
1R4L	Fenofibrate	-7.9	128.69 nM
	Binifibrate	-8.6	654.79 nM
	Bezafibrate	-8.6	583.43 nM
	Ciprofibrate	-6.8	40.76 µM
	Clofibrate	-5.6	14.26 µM
	Gemfibrozil	-7.1	59.78 µM
	Pioglitazone	-7.7	109.59 nM
	Rosiglitazone	-7.6	242.41 nM
	*Favipiravir	-5.6	84.49 µM
	*Chloroquine	-8.3	817.98 nM
	*Hydroxychloroquine	-8.1	14.26 µM
7MEQ	Fenofibrate	-6.6	16.87 µM
	Binifibrate	-6.1	1.18 µM
	Bezafibrate	-6.6	16.16 µM
	Ciprofibrate	-5.7	44.50 µM
	Clofibrate	-5.3	35.24 µM
	Gemfibrozil	-6.2	89.50 µM
	Pioglitazone	-6.1	38.29 µM
	Rosiglitazone	-7.1	22.73 µM
	*Favipiravir	-4.5	50.67 µM
	*Chloroquine	-6.0	523.00 µM
	*Hydroxychloroquine	-5.9	40.45 µM

Peroxisome proliferator-activated receptor (PPAR) agonists targeted drugs

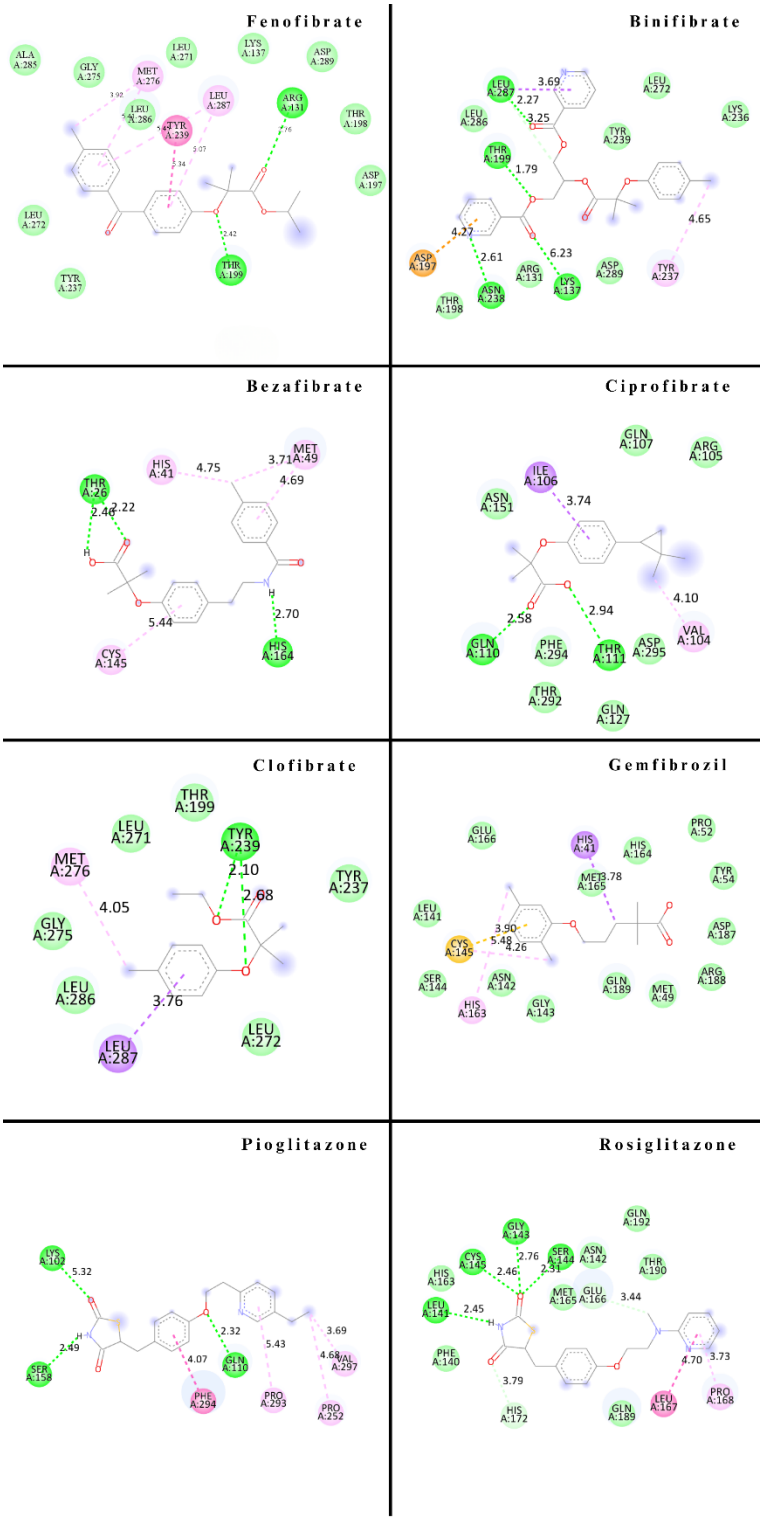

Figure 1. 2D binding interactions of target ligands on the active site of SARS-CoV-2 M^{pro} (PDB ID: 6LU7)

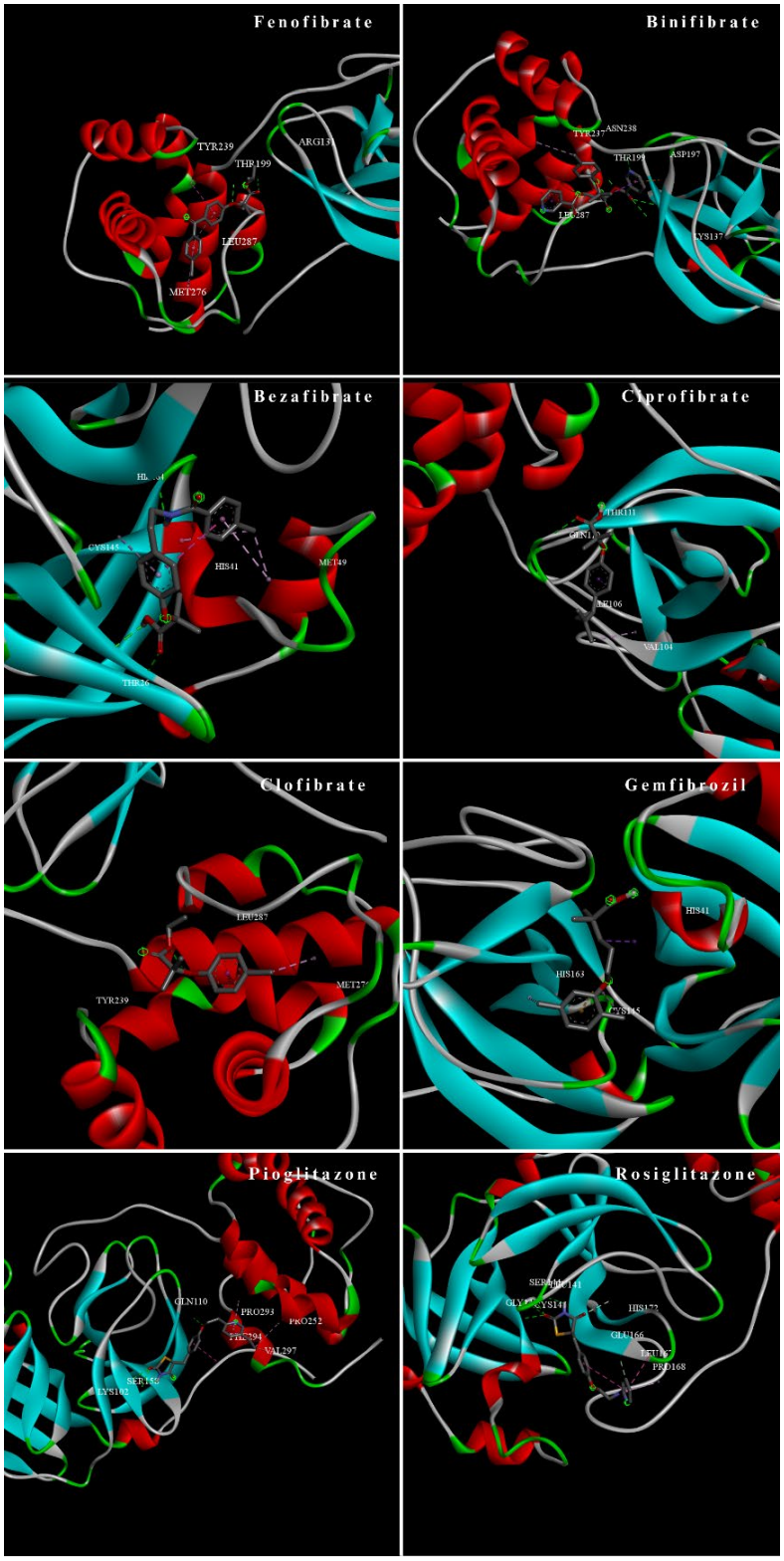

Figure 2. 3D binding interactions of target ligands on the active site of SARS-CoV-2 M^{pro} (PDB ID: 6LU7)

Peroxisome proliferator-activated receptor (PPAR) agonists targeted drugs

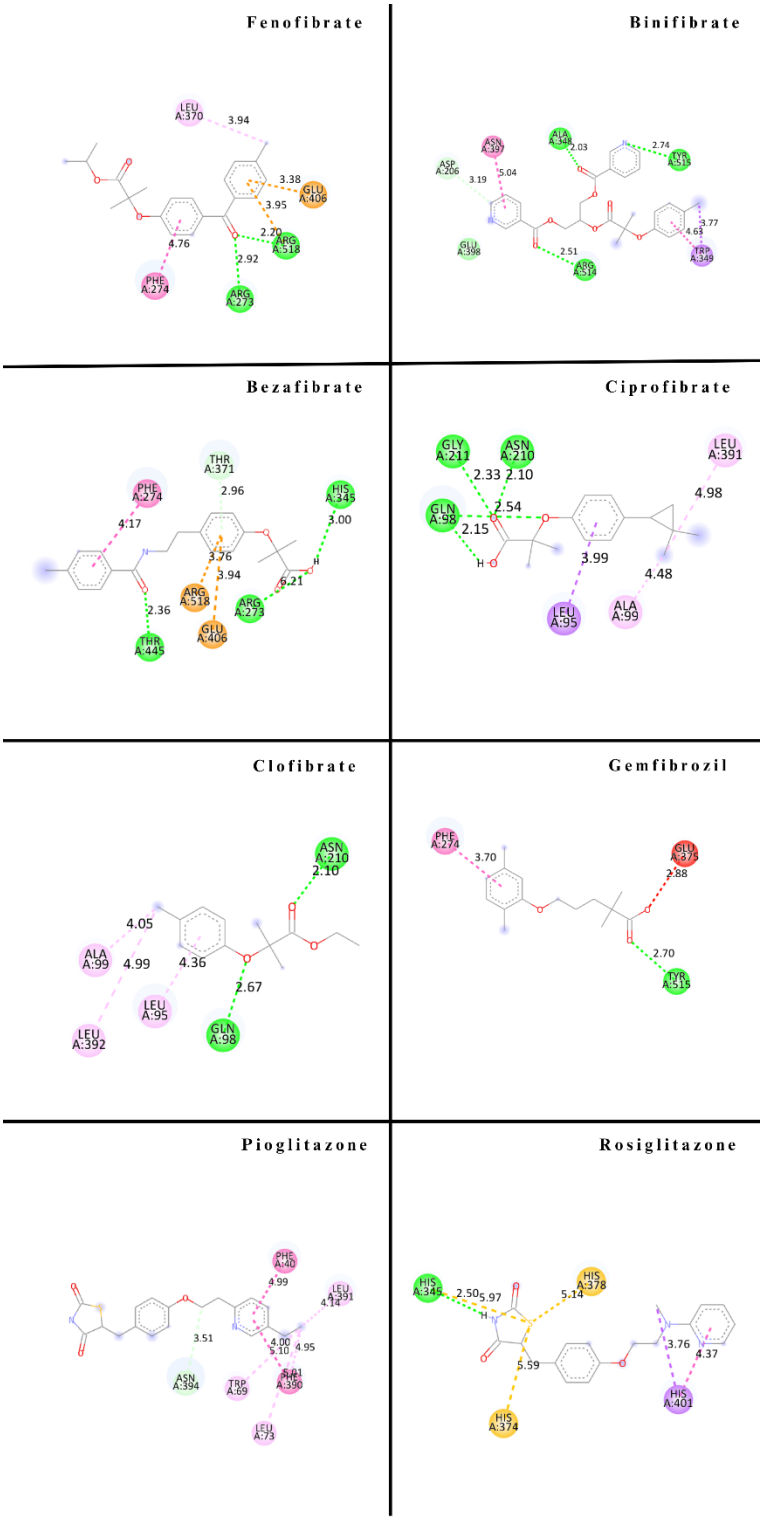

Figure 3. 2D binding interactions of target ligands on the active site of ACE2 (PDB ID: 1R4L)

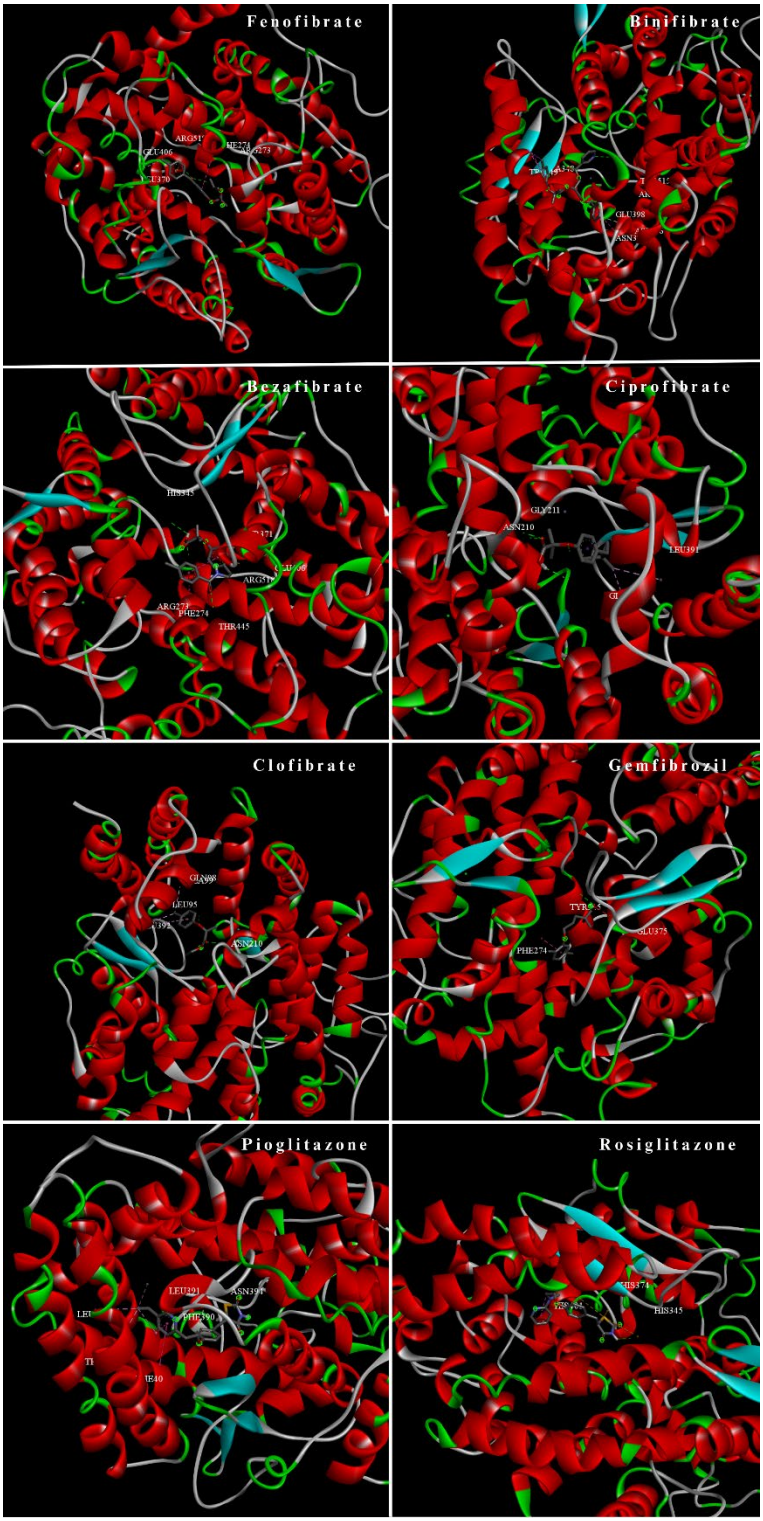

Figure 4. 3D binding interactions of target ligands on the active site of ACE2 (PDB ID: 1R4L)

Peroxisome proliferator-activated receptor (PPAR) agonists targeted drugs

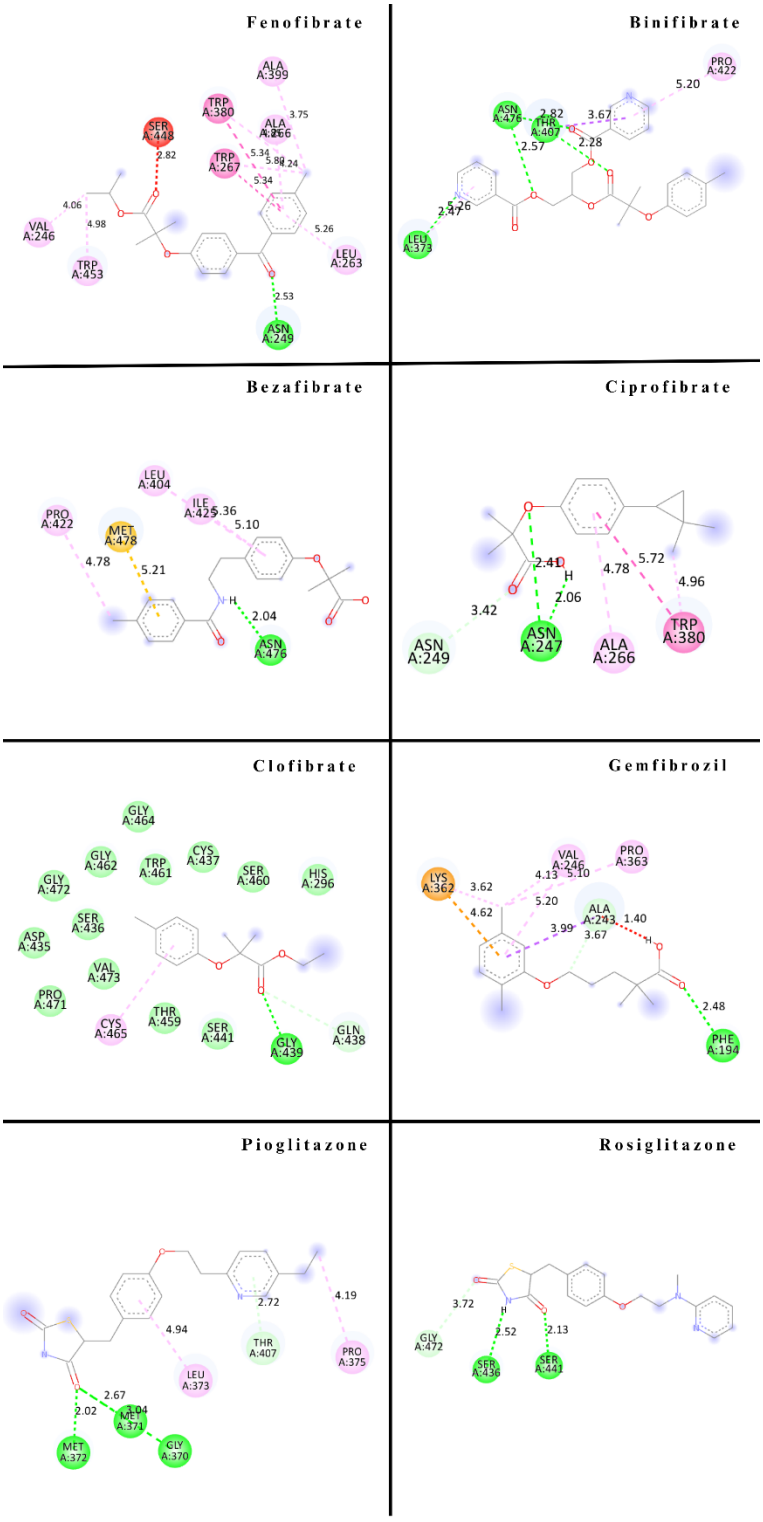

Figure 5. 2D binding interactions of target ligands on the active site of TMPRSS2 (PDB ID: 7MEQ)

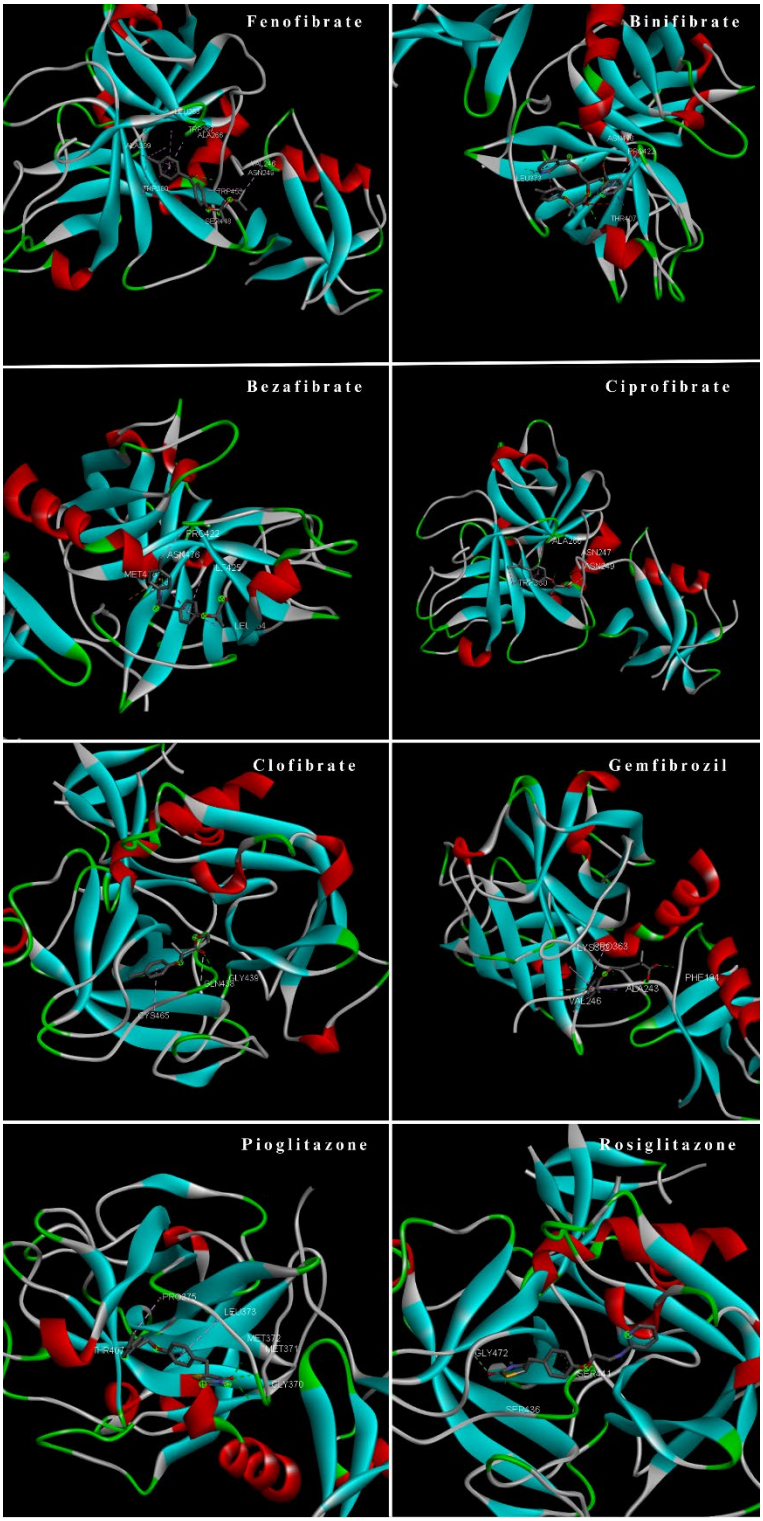

Figure 6. 3D binding interactions of target ligands on the active site of TMPRSS2 (PDB ID: 7MEQ)

Peroxisome proliferator-activated receptor (PPAR) agonists targeted drugs

The highest binding affinity results of rosiglitazone and fenofibrate compounds in SARS-CoV-2 M^{pro} (PDB ID: 6LU7) showed hydrophobic interactions with alkyl interactions with MET276 at distances of 3.92 and 5.41 Å, alkyl interactions with LEU287 at distances of 5.07 and 5.45 Å, and pi-alkyl interactions with TYR239 at a distance of 5.34 Å. These distances indicated that the fenofibrate compound can interact near the surface in the SARS-CoV-2 M^{pro} structure. In addition, vander walls interactions (amino acids LYS137, ASP197, THR198, TYR237, LEU271, LEU272, GLY275, ALA285, LEU286) also contribute to hydrophobic interactions. Hydrogen bonding interactions of fenofibrate compound also occurred at a distance of 2.76 Å with ARG131 and 2.42 Å with THR199. Hydrogen bonds also domanstrate stable binding to the protein. When the bond structures in the rosiglitazone compound were analysed, hydrophobic interactions of 3.73 Å (alkyl bond) with PRO168 and 4.70 Å (pi-alkyl bond) with LEU167 took place. Likewise, rosiglitazone compound contacted the protein structure with vander walls interactions (PHE140, ASN142, HIS163, THR190, GLN192) close to the surface. Rosiglitazone compound showed stable bonding ability at distances of 2.45 Å with LEU141, 2.76 Å with GLY143, 2.31 Å with SER144, 2.46 Å with CYS145, 3.44 with GLU166 and 3.79 Å with HIS172. When the results were evaluated, fenofibrate and rosiglitazone, potential compounds that can be used as alternatives to standard compounds in SARS-CoV2-M^{pro} structure, showed good binding properties.

Upon evaluating the binding potential of the fibrate derivatives binifibrate and bezafibrate with the ACE2 protein structure (PDB ID: 1R4L), binifibrate exhibited promising interactions at the active site. Specifically, π-alkyl interactions were observed between binifibrate and the residue THR349, with bond distances ranging from 3.77 to 4.63 Å. An alkyl interaction was also identified with ASN397 at a distance of 5.04 Å, contributing to hydrophobic stabilization within the binding pocket. In addition, van der Waals interactions were detected between binifibrate and GLU398, further supporting the binding affinity.

Stable hydrogen bonding interactions were a key feature of binifibrate's binding profile. These included a 3.19 Å hydrogen bond with ASP206, a 2.03 Å bond with ALA348, a 2.51 Å bond with ARG514, and a 2.74 Å bond with TYR515. Collectively, these interactions suggest that binifibrate has a strong and stable binding orientation within the ACE2 active site, potentially surpassing that of standard comparator drugs in terms of interaction profile and binding stability.

Molecular docking analyses targeting the TMPRSS2 protein (PDB ID: 7MEQ) revealed that fenofibrate and bezafibrate compounds exhibited higher binding affinity compared to standard drugs. Detailed evaluation of the binding interactions for the fenofibrate compound showed hydrophobic alkyl interactions with VAL246, ALA266, LEU263, ALA399, and TRP453 residues at distances ranging from 3.75 to 5.26 Å. Additionally, π-alkyl interactions were observed with TRP267 and TRP380 residues at distances between 4.24 and 5.34 Å.

In terms of hydrogen bonding, fenofibrate formed a stable hydrogen bond with ASN249 at a distance of 2.53 Å. These interactions suggest that fenofibrate may bind to TMPRSS2 with high specificity, potentially contributing to its strong binding affinity.

Table 2. Intermolecular interactions of selected drugs and standards against SARS-CoV-2 M^{pro} (PDB ID: 6LU7), ACE-2 (PDB ID: 1RL4), and TMPRSS2 (PDB ID: 7MEQ) by molecular docking study

Protein	Drugs	Hydrogen Bonding Interactions	Hydrophobic Interactions	Elecotrostatic Interactions
6LU7	Fenofibrate	ARG131, THR199	LYS137, ASP197, THR198, TYR237, LEU271, LEU272, GLY275, ALA285, LEU286, ASP289	-
	Binifibrate	LYS137, THR199, ASN238, LEU287	ARG131, THR198, LYS236, TYR237, TYR239, LEU286, LEU287, ASP289	ASP197
	Bezafibrate	THR26, HIS164	HIS41, MET49, CYS145	-
	Ciprofibrate	GLN110, THR111	VAL104, ARG105, ILE106, GLN107, GLN127, ASPN151, THR292, PHE294, ASP295	-
	Clofibrate	THR239	THR199, TYR237, LEU271, LEU272, GLY275, MET276, LEU286, LEU287	-
	Gemfibrozil	-	HIS41, MET49, PRO52, TYR54, LEU141, ASN142, GLY143, SER144, HIS164, MET165, GLU166, ASP187, ARG188, GLN189	CYS145
	Pioglitazone	LYS102, GLN110, SER158	PRO252, PRO293, PHE294, VAL297	-
	Rosiglitazone	LEU141, GLY143, SER144, CYS145, GLU166, HIS172	PHE140, ASN142, HIS163, MET165, LEU167, PRO168, GLN189, THR190, GLN192	-
	Fenofibrate	ARG273, ARG518	PHE274, LEU370	GLU406
	Binifibrate	ASP206, ALA348,	TRP349, ASN397, GLU398	-

Peroxisome proliferator-activated receptor (PPAR) agonists targeted drugs

1R4L		ARG514, THR515		
	Bezafibrate	ARG273, HIS345, THR371, THR445	PHE274	GLU406, ARG518
	Ciprofibrate	GLN98, ASN210, GLY211	LEU95, ALA99, LEU391	-
	Clofibrate	GLN98, ASN210	LEU95, ALA99, LEU392	-
	Gemfibrozil	THR515	PHE274	-
	Pioglitazone	ASN394	PHE40, TRP69, LEU73, PHE390, LEU391	-
	Rosiglitazone	HIS345	HIS401	HIS374, HIS378
7MEQ	Fenofibrate	ASN249	VAL246, LEU263, ALA266, TRP267, TRP380, ALA399, TRP453	-
	Binifibrate	LEU373, THR407, ASN476	PRO422	-
	Bezafibrate	ASN476	LEU404, PRO422, ILE425	MET478
	Ciprofibrate	ASN247, ASN249	ALA266, TRP380	-
	Clofibrate	GLN438, GLY439	HIS296, ASP435, SER436, CYS437, SER460, TRP461, GLY462, PRO471, GLY472, VAL473	-
	Gemfibrozil	PHE194, ALA243	ALA246, PRO363	LYS362
	Pioglitazone	GLY370, MET371, MET372, THR407	LEU373, PRO375	-
	Rosiglitazone	SER436, SER441, GLY472	-	-

Fenofibrate is a fibric acid derivative drug used for the treatment of severe hypertriglyceridemia.[37] The lipid-modifying effects of this drug are mediated by the activation of the nuclear transcription factor PPARα.[37,38] In a recent study, it was shown that fenofibate has some effects such as cardiovascular and renal protective.[39] At the same time, a study by Ehrlich et al. showed that the PPARα agonist fenofibrate reversed the metabolic changes induced by SARS-CoV-2 and inhibited viral replication in lung epithelial cells.[40] In the present molecular docking analysis, fenofibrate exhibited

strong binding affinity to SARS-CoV-2 main protease (6LU7, −6.4 kcal/mol) and ACE2 (1R4L, −7.9 kcal/mol), along with a significant interaction with TMPRSS2 (7MEQ, −6.6 kcal/mol).

Binifibrate is a PPARα agonist molecule derived from fibrate and was developed for the treatment of hyperlipidemia.[41-43] It was observed by Arun et al. that this drug binds strongly to the SARS-CoV-2 main protease.[44] Supporting this, our docking data revealed binifibrate as thepotent binder to TMPRSS2 (−6.1 kcal/mol) among the compounds investigated, and it also demonstrated substantial affinity toward ACE2 (−8.6 kcal/mol).

Bezafibrate is also a useful and well tolerated PPARα agonist in the treatment of dyslipidemia.[45,46] Bezafibrate was also found to reduce serum hepatitis C virus RNA levels in patients with complicated chronic hepatitis C with hyperlipidemia.[47] In this study, it ranked second in TMPRSS2 binding affinity (−6.6 kcal/mol) and matched binifibrate in ACE2 binding (−8.6 kcal/mol), suggesting potential for repurposing.

Ciprofibrate is PPARα agonist developed for use in the treatment of hyperlipidemia.[48,49] The contribution of this drug molecule to airway remodeling in a study on cigarette smoke-exposed rats suggests that it may have several different effects.[50] However, it exhibited the weakest binding to SARS-CoV-2 main protease (−6.0 kcal/mol), outperforming only favipiravir (−4.2 kcal/mol) among reference compounds.

Clofibrat is another PPARα agonist and hypolipidemic drug.[43,51] This drug has been studied for its different effects such as cardioprotective, neuroprotective, anticancer and antiinflammatory.[52-54] Clofibrat showed moderate binding to SARS- CoV-2 main protease, ACE2 and TMPRSS2 among the drugs studied. Similarly, gemfibrozil is a fibric acid derivative, a PPARα agonist drug. As with other PPARα agonists, this drug is also used in the treatment of hyperlipidemia.[55] In addition, gemfibrozil is effective in controlling dyslipidemia associated major coronery disease.[56] Gemfibrozil showed the lowest binding to ACE2 (-5.76 kcal/mol) and TMPRSS2 (-5.52 kcal/mol) in which this drug might not be a good lead molecule for our purpose in the development of anti-CoV drug design studies.

Pioglitazone, a thiazdolidindione derivative, activates PPARγ receptors and reduces insulin resistance and is used in the treatment of type 2 diabetes.[57] Pioglitazone, an old diabetes drug, has recently shown efficacy in ameliorating nonalcoholic steatohepatitis.[58] At the same time, the efficacy of this drug for coronary diseases has been observed.[59] In our study, pioglitazone demonstrated the high binding affinity to ACE2 (−7.7 kcal/mol) and strong interaction with SARS-CoV-2 main protease (−6.5 kcal/mol), implying promising potential as a lead compound in anti-COVID-19 drug development.

Rosiglitazone, another thiazolidinedione derivative, also acts as a PPARγ agonist.60 This drug was developed to lower blood sugar in patients with type 2 diabetes.61 It ranked the best in terms of binding energy to SARS-CoV-2 main protease (−6.8 kcal/mol) and ACE2 (−7.6 kcal/mol), further highlighting its repurposing potential.

Overall, rosiglitazone exhibited strong binding across targets, while binifibrate and bezafibrate were particularly notable for their ACE2 affinities. Fenofibrate and bezafibrate also demonstrated favorable interactions with TMPRSS2. However, the limited use of binifibrate due to its high potential for side effects reduces its effectiveness. These results provide preliminary information for the evaluation of these drug molecules and other drugs with similar chemical structures in the treatment of COVID-19.

4. Conclusion

COVID-19 represents a pervasive global health challenge characterized by high morbidity and mortality and, to date, lacks a universally approved antiviral therapy. In the present study, we employed molecular docking to assess the affinity of selected peroxisome proliferator-activated receptor (PPAR) agonists against three critical proteins involved in SARS-CoV-2 infection: the main protease (Mpro; PDB ID: 6LU7), the angiotensin-converting enzyme 2 receptor (ACE2; PDB ID: 1R4L), and the serine protease TMPRSS2 (PDB ID: 7MEQ). Binifibrate and rosiglitazone emerged as particularly promising, displaying binding energies of −6.7 and −6.8 kcal/mol toward Mpro and of −8.6 and −7.6 kcal/mol toward ACE2, respectively, values that rival those of standard reference compounds. Additionally, bezafibrate and fenofibrate demonstrated strong interactions with TMPRSS2 (binding energies of −6.6

and −6.6 kcal/mol, respectively). These findings suggest that PPAR-targeted fibrates and thiazolidinediones possess the structural and energetic characteristics necessary for further optimization as lead candidates in anti-COVID-19 drug discovery.

ORCID

Suleyman Akocak: 0000-0003-4506-5265
Erkan Öner: 0000-0002-6332-6484
Gökçenur Gürbüz: 0009-0004-8816-5949
Nebih Lolak: 0000-0003-0578-2761

References

[1] Lu, H.; Stratton, C.W.; Tang, Y.W. Outbreak of pneumonia of unknown etiology in Wuhan, China: The mystery and the miracle. *J. Med. Virol*. **2020**, *92*, 401-402.
[2] Zhou, P.; Yang, X.L.; Wang, X.G.; Hu, B.; Zhang, L.; Zhang, W.; S. H.R.; Zhu, Y.; Li, B.; Huang, C.L. et al. A pneumonia outbreak associated with a new coronavirus of probable bat origin. *Nature* **2020**, *579*, 270-273.
[3] Chen, N.; Zhou, M.; Dong, X.; Qu, J.; Gong, F.; Han, Y.; Qiu, Y.; Wang, J.; Liu, Y.; Wei, Y. et al. Epidemiological and clinical characteristics of 99 cases of 2019 novel coronavirus pneumonia in Wuhan, China: a descriptive study. *Lancet* **2020**, *395*, 507-513.
[4] Steffens, I. A hundred days into the coronavirus disease (COVID-19) pandemic. *Euro Surveill*. **2020**, *25*, 2000550.
[5] WHO. COVID-19 Weekly Epidemiological Update Report. World Health Organization; 4 Nov 2022. p. 1-2.
[6] Li, F. Structure, function, and evolution of coronavirus spike proteins. *Annu. Rev. Virol*. **2016**, *3*, 237-261.
[7] Kirtipal, N.; Bharadwaj, S.; Kang, S.G. From SARS to SARS-CoV-2, insights on structure, pathogenicity and immunity aspects of pandemic human coronaviruses. *Infect. Genet. Evol*. **2020**, *85*, 104502.
[8] Bosch, B.J.; van der Zee, R.; de Haan, C.A.; Rottier, P.J. The coronavirus spike protein is a class I virus fusion protein: structural and functional characterization of the fusion core complex. *J. Virol*. **2003**, *77*, 8801-11.
[9] Hoffmann, M.; Kleine-Weber, H.; Schroeder, S.; Kruger, N.; Herrler, T.; Erichsen, S.; Schiergens, T.S.; Herrler, G.; Wu, N.H.; Nitsche, A. et al. SARS-CoV-2 cell entry depends on ACE2 and TMPRSS2 and is blocked by a clinically proven protease inhibitor. *Cell* **2020**, *181*, 271- 280.e8.
[10] Wrapp, D.; Wang, N.; Corbett, K.S.; Goldsmith, J.A.; Hsieh, C.L.; Abiona, O.; Graham, B.S.; MClellan, J:S. Cryo-EM structure of the 2019-nCoV spike in the prefusion conformation. *Science* **2020**, *367*, 1260-1263.
[11] Hamming, I.; Timens, W.; Bulthuis, M.L.; Lely, A.T.; Navis, G.; van Goor, H. Tissue distribution of ACE2 protein, the functional receptor for SARS coronavirus. A first step in understanding SARS pathogenesis. *J. Pathol*. **2004**, *203*, 631-7.
[12] Sasaki, M.; Uemura, K.; Sato, A.; Toba, S.; Sanaki, T.; Maenaka, K.; Hall, W.W.; Orba, Y.; Sawa, H.. SARS-CoV-2 variants with mutations at the S1/S2 cleavage site are generated in vitro during propagation in TMPRSS2-deficient cells. *PLoS. Pathog*. **2021**, *17*, e1009233.
[13] Senapati, S.; Banerjee, P.; Bhagavatula, S.; Kushwaha, P.P.; Kumar, S. Contributions of human ACE2 and TMPRSS2 in determining host-pathogen interaction of COVID-19. *J. Genet*. **2021**, *100*, 12.
[14] Shulla, A.; Heald-Sargent, T.; Subramanya, G.; Zhao, J.; Perlman, S.; Gallagher, T. A transmembrane serine protease is linked to the severe acute respiratory syndrome coronavirus receptor and activates virus entry. *J. Virol*. **2011**, *85*, 873- 82.
[15] Cheng, H.S.; Tan, W.R.; Low, Z.S.; Marvalim, C.; Lee, J.Y.H.; Tan, N.S. Exploration and development of PPAR modulators in health and disease: an update of clinical evidence. *Int. J. Mol. Sci*. **2019**, *20*, 5055.
[16] Mirza, A.Z.; Althagafi, I.I.; Shamshad, H. Role of PPAR receptor in different diseases and their ligands: Physiological importance and clinical implications. *Eur. J. Med. Chem*. **2019**, *166*, 502-513.
[17] Montaigne, D.; Butruille, L.; Staels, B. PPAR control of metabolism and cardiovascular functions. *Nat. Rev. Cardiol*. **2021**, *18*, 809-823.
[18] Dayspring, T.; Pokrywka, G. Fibrate therapy in patients with metabolic syndrome and diabetes mellitus. *Curr. Atheroscler. Rep*. **2006**, *8*, 356-64.
[19] Katsiki, N.; Nikolic, D.; Montalto, G.; Banach, M.; Mikhailidis, D.P.; Rizzo, M. The role of fibrate treatment in dyslipidemia: an overview. *Curr. Pharm. Des*. **2013**, *19*, 3124-31.

[20] Nanjan, M.J.; Mohammed, M.; Prashantha Kumar, B.R.; Chandrasekar, M.J.N. Thiazolidinediones as antidiabetic agents: A critical review. *Bioorg. Chem*. **2018**, *77*, 548-567.

[21] De Lellis, L.; Cimini, A.; Veschi, S.; Benedetti, E.; Amoroso, R.; Cama, A.; Ammazzalorso, A. The anticancer potential of peroxisome proliferator-activated receptor antagonists. *Chem. Med. Chem*. **2018**, *13*, 209-219.

[22] Ammazzalorso, A.; De Lellis, L.; Florio, R.; Bruno, I.; Filippis, B.D.; Fantacuzzi, M.; Giampietro, L.; Maccallini, C.; Perconti, S.; Verginelli, F. Cytotoxic effect of a family of peroxisome proliferator-activated receptor antagonists in colorectal and pancreatic cancer cell lines. *Chem. Biol. Drug Des*. **2017**, *90*, 1029-1035.

[23] Pushpakom, S.; Iorio, F.; Eyers, P.A.; Escott, P:A.; Hopper, S.; Wells, A., Doig, A.; Guilliams, T.; Latimer, J.; McNamee, C. et al. Drug repurposing: progress, challenges and recommendations. *Nat. Rev. Drug Discov*. **2019**, *18*, 41-58.

[24] Eleftheriou, P.; Amanatidou, D.; Petrou, A.; Geronikaki, A. In silico evaluation of the effectivity of approved protease inhibitors against the main protease of the novel SARS-CoV-2 Virus. *Molecules* **2020**, *25*, 2529.

[25] Sencanski, M.; Perovic, V.; Pajovic, S.B.; Adzic, M.; Paessler, S.; Glisic, S. Drug repurposing for candidate SARS-CoV-2 main protease inhibitors by a novel *in silico* method. *Molecules* **2020**, *25*, 3830.

[26] Ferrari, I.V. Blind docking analysis of potential drugs against SARS-COV-1 and SARS-COV-2 proteins.*IJSRCSE*. **2021**, *9*, 85-89.

[27] Zhang, L.; Lin, D.; Sun, X.; Curth, U.; Drosten, C.; Sauerhering, L.; Becker, S.; Rox, K.; Hilgenfeld, R. Crystal structure of SARS-CoV-2 main protease provides a basis for design of improved α-ketoamide inhibitors. *Science* **2020**, *368*, 409-412.

[28] Anand, K.; Ziebuhr, J.; Wadhwani, P.; Mesters, J.R.; Hilgenfeld, R. Coronavirus main proteinase ($3CL^{pro}$) structure: Basis for design of anti-SARS drugs. *Science* **2003**, *300*, 1763–1767.

[29] Jin, Z.; Du, X.; Xu, Y.; Deng, Y.;Liu, M.; Zhao, Y.; Zhang, B.; Li, X.; Zhang, L.; Peng, C. et.al. The crystal structure of COVID-19 main protease in complex with an inhibitor N3. *Nature* **2020**, *582*, 289-293

[30] Towler, P.; Staker, B.; Prasad, S.G.; Menon, S.; Tang, J.; parsons, T.; Ryan, D.; Fisher, M.; Williams, D.; Dales, N.A. et al.. Inhibitor bound human Angiotensin Converting Enzyme-Related Carboxypeptidase (ACE2). *J. Biol. Chem*. **2004** , *279*, 17996-8007.

[31] Fraser, B.J.; Beldar, S.; Seitova, A.; Hutchinson, A.; Mannar, D.; Li, Y.; Kwon, D.; Wilson, R.P.; Leopold, K.; Subramaniam S. et al. Crystal structure of human TMPRSS2 in complex with Nafamostat. *Nat. Chem. Biol*. **2022**, *18*, 963-971.

[32] Lolak, N.; Akocak, S.; Turkes, C.; Taslimi, P.; Isık, M.; Beydemir Ş.; Gulçin, İ.; Durgun, M. Synthesis, characterization, inhibition effects, and molecular docking studies as acetylcholinesterase, α-glycosidase, and carbonic anhydrase inhibitors of novel benzenesulfonamides incorporating 1,3,5-triazine structural motifs. *Bioorg. Chem*. **2020**, *100*, 103897.

[33] Lolak, N.; Boga, M.; Sonmez, G. D.; Tuneg, M.; Doğan, A.; Akocak, S. *In silico* studies and DNA cleavage, antioxidant, acetylcholinesterase, and butyrylcholinesterase activity evaluation of bis-histamine schiff bases and bis-spinaceamine substituted derivatives. *Pharm. Chem. J*. **2022**, *55*, 1338-1344.

[34] Koyuncu, I.; Durgun, M.; Yorulmaz, N.; Toprak S.; Gonel, A.; BAyraktar, N.; Çağlayan, A. Molecular docking demonstration of the liquorice chemical molecules on the protease and ACE2 of COVID-19 virus. *Curr. Enz. Inhibition*. **2021**, *17*, 98-110.

[35] Doğan, A.; Şengül, F.; Lolak, N.; Akocak, S. *In silico* molecular docking study on selective cyclooxygenase-2 inhibitor drugs for SARS-Cov-2 active main protease. *Nov. Appro. Drug. Des. Dev.* **2022**, *6(3)*, 555686.

[36] Dogan, A.; Yanilmaz, E. M. B.; Karakoc, G.; Parlar, A.; Annaç, E.; Lolak, N.; Akocak, S. Investigating the anti-inflammatory potential of SLC-0111: a carbonic anhydrase inhibitor targeting cyclooxygenase-mediated inflammatory pathways in a carrageenan-induced rat model. *J. Biochem. Mol. Toxic.* **2025**, *39(3)*, e70217.

[37] Oscarsson, J.; Önnerhag, K.; Risérus, U.; Sunden, M.; JOhansson, L.; Jansson, P.A.; Moris, L.; Nilson, P.M.; Erikson, J.W.; Lind. L. Effects of free omega-3 carboxylic acids and fenofibrate on liver fat content in patients with hypertriglyceridemia and non-alcoholic fatty liver disease: A double-blind, randomized, placebo- controlled study. *J. Clin. Lipidol*. **2018**, *12*, 1390-1403.

[38] Feng, X.; Gao, X.; Jia, Y.; Zhang, H.; Xu, Y.; Wang, G. PPAR-α agonist fenofibrate decreased RANTES levels in type 2 diabetes patients with hypertriglyceridemia. *Med. Sci. Monit*. **2016**, *22*, 743-51.

[39] Balakumar, P.; Sambathkumar, R.; Mahadevan, N.; Muhsinah, A.B.; Alsayari, A.; Venkateswaramurthy, N.; Dhanaraj, A.A. Molecular targets of fenofibrate in the cardiovascular-renal axis: A unifying perspective of its pleiotropic benefits. *Pharmacol. Res*. **2019**, *144*, 132-141.

[40] Ehrlich, A.; Uhl S.; Ioannidis, K.; Hofree, M.; ten Oever, B.R.; Nahmias, Y. The SARS- CoV-2

transcriptional metabolic signature in lung epithelium. *SSRN Electron J*. **2020**. doi: 10.2139/ssrn.3650499.

[41] Labios, M.; Martínez, M.; Vayá, A.; Gabriel, F.; Guiral, V.; Aznar, J. Effect of a modified fibrate (Biniwas Retard) on hemorheological alterations in hyperlipemic patients. *Clin. Hemorheol. Microcirc*. **1999**, *21*, 79-85.

[42] Corominas Vilardell, A.; de Oya Otero, M.; Escobar Jiménez, F.; Anguera Vila, A. Multicenter clinical, double blind, and randomized study to assess the effectiveness and safety of binifibrate versus gemfibrozil in type IIa, IIb, and IV hyperlipidemia. *An. Med. Int.* **1993**, *10*, 537-41.

[43] Montastruc, F.; Benevent, J.; Rousseau, V.; Durrieu, G.; Sommet, A.; Montastruc, J.L. Risk of diabetes with fibrates and statins: a pharmacoepidemiological study in VigiBase®. *Fundam. Clin. Pharmacol*. **2019**, *33*, 108-112.

[44] Arun, K.G,; Sharanya, C.S.; Abhithaj, J.; Francis, D.; Sadasivan, C. Drug repurposing against SARS-CoV-2 using E-pharmacophore based virtual screening, molecular docking and molecular dynamics with main protease as the target. *J. Biomol. Struct. Dyn*. **2021**, *39*, 4647-4658.

[45] Heller F.; Harvengt C. Effects of clofibrate, bezafibrate, fenofibrate and probucol on plasma lipolytic enzymes in normolipaemic subjects. *Eur. J. Clin. Pharmacol*. **1983**, *25*, 57- 63.

[46] Cabrero, A.; Alegret, M.; Sánchez, R.M.; Adzet, T.; Laguna, J.C.; Vázquez, M. Bezafibrate reduces mRNA levels of adipocyte markers and increases fatty acid oxidation in primary culture of adipocytes. *Diabetes* **2001**, *50*, 1883-90.

[47] Fujita, N.; Kaito, M.; Kai, M.; Sugimoto, R.; Tanaka, H.; Horiike, S.; Konishi, M.; Iwasa, M.; Watanabe, S.; Adachi, Y. Effects of bezafibrate in patients with chronic hepatitis C virus infection: Combination with interferon and ribavirin. *J. Viral Hepat*. **2006**, *13*, 441–448.

[48] Bruckert, E.; Dejager, S.; Chapman, M.J. Ciprofibrate therapy normalises the atherogenic low density lipoprotein subspecies profile in combined hyperlipidemia. *Atherosclerosis* **1993**, *100*, 91-102.

[49] Turay, J.; Grniaková, V.; Valka, J. Changes in paraoxonase and apolipoprotein A- I, B, C-III and E in subjects with combined familiar hyperlipoproteinemia treated with ciprofibrate. *Drugs Exp. Clin. Res*. **2000**, *26*, 83-8.

[50] Ke, Q.; Yang, L.; Cui, Q.; Diago, W.; Zhang, Y.; Xu, M., He, B. Ciprofibrate attenuates airway remodeling in cigarette smoke-exposed rats. *Respir. Physiol. Neurobiol*. **2020**, *271*, 103290.

[51] Kadota, Y.; Kazama, S.; Bajotto, G.; Kitaura, Y.; Shimomura, Y. Clofibrate-induced reduction of plasma branched-chain amino acid concentrations impairs glucose tolerance in rats. *JPEN J. Parenter. Enteral. Nutr*. **2012**, *36*, 337-43.

[52] Oyagbemi, A.A.; Adebiyi, O.E.; Adigun, K.O.; Ogunpolu, B.S.; Falayi, O.O.; Hassan, H.O.; Folarin, A.R.; Adebayo, A.K; Adejumobi, O.A.; Asenuga, E. R. et al. Clofibrate, a PPAR-α agonist, abrogates sodium fluoride-induced neuroinflammation, oxidative stress, and motor incoordination via modulation of GFAP/Iba-1/anti-calbindin signaling pathways. *Environ. Toxicol*. **2020**, *35*, 242-253.

[53] Ibarra-Lara, L.; Sánchez-Aguilar, M.; Soria-Castro, E.; Vargas-Barron, J.; Roldan, F.J.; Pavon, N.; Torres_Narvaez, J.C.; Cervantes-Pereze, L.G.; Pastelin-Hernandez, G.; Sanches-Mendoza, A. Clofibrate treatment decreases inflammation and reverses myocardial infarction-induced remodelation in a rodent experimental model. *Molecules* **2019**, *24*, 270.

[54] Wang, S.; Hannafon, B.N.; Zhou, J.; Ding, W.Q. Clofibrate induces heme oxygenase 1 expression through a PPARα-independent mechanism in human cancer cells. *Cell Physiol. Biochem*. **2013**, *32*, 1255-64.

[55] Jana, M.; Mondal, S.; Gonzalez, F.J.; Pahan, K. Gemfibrozil, a lipid-lowering drug, increases myelin genes in human oligodendrocytes via peroxisome proliferator-activated receptor-β. *J. Biol. Chem*. **2012**, *287*, 34134-48.

[56] Doggrell, S.A. Gemfibrozil prevents major coronary events by increasing HDL- cholesterol and more. *Expert. Opin. Pharmacother*. **2001**, *2*, 1187-9.

[57] Nagashima, K.; Lopez, C.; Donovan, D.; Ngai, C.; Fontanez, N.; Bensadoun, A.; Fruchart-Najib, J.; Holleran, S.; Cohn, J.S.; Ramakrishnan, R.; Ginsberg, H.N. Effects of the PPARgamma agonist pioglitazone on lipoprotein metabolism in patients with type 2 diabetes mellitus. *J. Clin. Invest*. **2005**, *115*, 1323-32.

[58] Cusi, K.; Orsak, B.; Bril, F.; Lomonaco, R.; Hect, J.; Ortiz-Lopez, C.; Tio, F.; Hardies, J.; Darland, C.; Musi, N. et.al. Long-term pioglitazone treatment for patients with nonalcoholic steatohepatitis and prediabetes or type 2 diabetes mellitus: A randomized trial. *Ann. Intern. Med*. **2016**, *165*, 305- 15.

[59] Nissen, S.E.; Nicholls, S.J.; Wolski, K.; et al. Comparison of pioglitazone vs glimepiride on progression of coronary atherosclerosis in patients with type 2 diabetes: the PERISCOPE randomized controlled trial. *JAMA*. **2008**, *299*, 1561-1573.

[60] Camp, H.S.; Li, O.; Wise, S.C.; et al. Differential activation of peroxisome proliferator-activated receptor-gamma by troglitazone and rosiglitazone. *Diabetes* **2000**, *49*, 539-47.

[61] Nissen, S.E.; Wolski, K. Effect of rosiglitazone on the risk of myocardial infarctionand death from cardiovascular causes. *N. Engl. J. Med*. **2007**, *14*, 356:2457-71.